IDENTIFYING HEAD-TRUNK AND LOWER LIMB CONTRIBUTIONS TO GAZE STABILIZATION DURING LOCOMOTION

Mulavara P Ajitkumar[1]; Bloomberg J Jacob[2]

[1]National Space Biomedical Research Institute, Bobby R. Alford Department of Otorhinolaryngology and Communicative Sciences, Baylor College of Medicine, Houston, TX 77030, [2]Neuroscience Laboratories, NASA, Johnson Space Center, Houston, TX 77058, USA

Primary Corresponding Author:

Ajitkumar P. Mulavara, Ph.D.

Mailing Address –

NASA/Johnson Space Center
Neuroscience Laboratories
2101 NASA Road 1, MC: SK3
Houston, TX 77058

Tel. 281 483 8994
Fax. 281 244 5734
email : amulavar@ems.jsc.nasa.gov

Abstract

The goal of the present study was to determine how the multiple, interdependent full-body sensorimotor subsystems respond to a change in gaze stabilization task constraints during locomotion. Nine subjects performed two gaze stabilization tasks while walking at 6.4 km/hr on a motorized treadmill: 1) focusing on a central point target; 2) reading numeral characters; both presented at 2m in front at the level of their eyes. While subjects performed the tasks we measured: temporal parameters of gait, full body sagittal plane segmental kinematics of the head, trunk, thigh, shank and foot, accelerations along the vertical axis at the head and the shank, and the vertical forces acting on the support surface. We tested the hypothesis that with the increased demands placed on visual acuity during the number recognition task, subjects would modify full-body segmental kinematics in order to reduce perturbations to the head in order to successfully perform the task. We found that while reading numeral characters as compared to the central point target: 1) compensatory head pitch movement was on average 22% greater despite the fact that the trunk pitch and trunk vertical translation movement control were not significantly changed; 2) coordination patterns between head and trunk as reflected by the peak cross correlation between the head pitch and trunk pitch motion as well as the peak cross correlation between the head pitch and vertical trunk translation motion were not significantly changed; 3) knee joint total movement was on average 11% greater during the period from the heel strike event to the peak knee flexion event in stance phase of the gait cycle; 4) peak acceleration measured at the head was significantly reduced by an average of 13% in four of the six subjects. This was so even when the peak acceleration at the shank and the transmissibility of the shock wave

at heel strike (measured by the peak acceleration ratio of the head/shank) remained unchanged. Taken together these results provide further evidence that the full body contributes to gaze stabilization during locomotion, and that its different functional elements can be modified online to contribute to gaze stabilization for different visual task constraints.

1. Introduction

Maintaining gaze stabilization during locomotion places substantial demands on multiple sensorimotor systems for precise coordination. Previously, gaze stabilization during locomotion has been studied almost exclusively as a problem of eye-head or eye-head-trunk coordination (1-4). However, locomotion involves cyclical physical interactions, consisting of impacts, with the environment. Hence, focusing on a target and maintaining visual acuity during these activities may require a mechanism or mechanisms to regulate or manage the energy flow from interfering with the visual and vestibular sensory transduction that contribute to gaze stabilization (5). Thus, stabilization of visual images during natural body movement such as locomotion requires full-body coordination of the eye-head and head-trunk systems combined with the lower limb apparatus. From this point of view, the whole body is an *integrated* gaze stabilization system, in which several subsystems contribute to gaze stabilization and accurate visual acuity during body motion.

Eye-Head Coordination During Locomotion

The eyes must be stabilized in space for clear vision during head movement. The vestibulo-ocular reflex (VOR) makes a major contribution to gaze stabilization by generating compensatory eye movements in response to angular head rotation. However the gain of the VOR is never quite ideal (1.0) for stabilization of images of distant targets. Pitch and yaw VOR gain can average 0.98 during passive head movements, but when the body is in motion, pitch and yaw VOR gain decreases (6). During walking, VOR gain in pitch remains quite accurate (0.97), but is significantly decreased in yaw (0.80). During running, VOR gain in pitch and yaw can be as low as 0.75 (7). Because natural head

movements have high frequency components, retinal image slip velocity can be sufficient to degrade visual acuity during activities like walking and running (8). Hence, additional strategies must be employed by the head-trunk complex and the lower limbs to stabilize gaze when the body is in motion.

Head-Trunk Coordination During Locomotion

Coordination between the head and trunk segments have been extensively studied and have been shown to aid in dynamic equilibrium control and gaze stabilization functions while walking (for review see 5,9). These studies have hypothesized the use of the head as a stabilized inertial guidance platform during complex body movements. Such a platform may help provide a stable reference frame to coordinate body movements while performing various motor tasks (for a detailed review see 10). Head stabilization also helps focusing on a target and in maintaining visual acuity for navigational control through a cluttered environment during locomotion. The restriction of head angular motion aids gaze stability by reducing the ocular compensation needed to maintain gaze on a fixed target (11). In this respect, empirical evidence has shown that during walking and running the peak angular velocities of the head, in each plane of rotation, were generally below held below 100 deg/sec (12) which is well below the saturation velocity of 360 deg/sec of the vestibular ocular reflex (13). We have shown along with other investigators that the angular head movements may actually contribute to gaze stabilization during locomotion. An example of this is the head rotation in the flexion-extension plane (as in nodding the head) that compensates for the vertical translation of the trunk that occurs with each step during the gait cycle (1,3,4,14-16). The

magnitude of the head rotations was observed to be controlled and also dependent on the distance of the visual target (3,16). Thus, the goal-directed response of these head movements during concurrent locomotion and visual target fixing suggests that head movements are not completely dependent on passive inertial and visco-elastic properties of the head-neck system but may be actively modulated to respond to altered gaze control requirements.

Modulation Of Shockwave Transmission During Locomotion By The Lower limb

During locomotion, the foot strikes the ground twice during each gait cycle. The impact of these heel-strikes results in transmission of vertical shock along body segments, from the foot to the head (17,18). Foot contact with the ground is a critical phase of locomotion, as the forces arising from the foot-ground interaction can challenge the visual and vestibular systems (5,14,15, 19). The musculoskeletal system impedes, directs and dissipates this energy (for review see 5). However, these forces create vibrations, which, if unattenuated, could interfere with the visual-vestibular sensory systems in the head (15,20). The body controls these vibrations: muscles and joints act as filters to minimize the perturbing effects of impacts with the ground and help to maintain a stable trajectory at the head (21). While studying forces acting on the head with respect to the trunk, work in our laboratory has previously shown that head movement control is also modulated depending on the events, such as the high impact and the low/no impact phases, occurring during the gait cycle (22).

Thus, appropriate attenuation of energy transmission during locomotion, achieved by the modulation of the lower limbs joint configuration coupled with appropriate eye-

head-trunk coordination strategies, form the fundamental features of an integrated gaze stabilization system. Therefore, the long-term goal of our current series of experiments is to determine how the multiple, interdependent full-body sensorimotor subsystems aiding gaze stabilization during locomotion are functionally coordinated and adaptively modified. The goal of the present study was to determine how modification of a gaze stabilization task induces modulation in function of the head-trunk complex and the lower limb apparatus. Subjects walked on a treadmill while either visually fixating a point target or while performing a number recognition task. We hypothesized that imposing a gaze stabilization task with increased demand for visual acuity (i.e. the number recognition task) would: 1) modify head movement control and head-trunk coordination during locomotion; and 2) modify lower limb joint configurations during the high impact phases of the gait cycle to reduce the amplitude of the shock-wave transmitted to the head. This would demonstrate that multiple whole-body systems contribute to gaze stabilization and that they can be flexibly modified in response to changing gaze task constraints.

2. Methods

Subjects

Nine subjects, four males and 5 females, average (± one standard error of mean, SEM) height of 169.11 (± 2.35) cm, weight 65.67 (± 2.77) Kg, with no history of neurologic, otologic, cardiovascular or significant orthopedic disorders participated in this experiment. All subjects were competent to give informed consent and these were obtained from each subject before participation in this study. All subjects were volunteers recruited through the Johnson Space Center Human Test Subject Facility.

Locomotion Gaze Stablization Protocol

Each subject wore cycling shorts, a sleeveless shirt and the same brand of running shoe. Subjects walked on a motorized treadmill at 6.4 km/h while performing two goal-directed gaze stabilization tasks that required them to 1) focus on a central point target (DOT); or 2) read numeral characters presented centrally on a laptop computer (NRT). During testing, the laptop was placed on a tripod at the subject's eye level at a distance of two meters. Microsoft Power Point™ slide presentation software was used to display numbers for the gaze stabilization task that was performed during treadmill locomotion. Ten slides presenting five numbers of one font size appeared white on a black background in succession. Font sizes ranged from 12 to 20 point in increments of two points. The presentations of the five font sizes were randomized, with each font size presented in two different slides. These font sizes, at two meters, correspond to a range of visual acuity of 20/15 to 20/30 on a traditional Snellen eye chart, encompassing most subjects' static visual acuity. Numerals were balanced among integers from 0-9 such that each integer was presented an equal number of times. The Geneva font was chosen for its uncomplicated number design. Each slide was visible for three seconds. The brightness and contrast were maximized with room lighting held constant. For the number recognition task subjects were asked to read aloud the numbers presented in each slide while walking. A test operator recorded responses during the test. Each gaze stabilization task was repeated over three 20 sec trials. Subjects were permitted to rest between trials. During testing, all subjects wore a safety harness attached to an overhead frame to prevent injury resulting from a fall. Downward movement of the harness 15.24 cm in the -Z direction (i.e. a fall) would result in activation of the treadmill "stop" switch.

This harness provided no support during nominal performance and did not interfere with the natural movements of the head or limbs. A "spotter" also monitored subjects at all times to ensure their safety.

While subjects walked on the treadmill and performed the two gaze stabilization tasks we measured: 1) full body 3-dimensional kinematic data using a video-based motion analysis system (Motion Analysis Corp., Santa Rosa, CA); 2) the shock-wave transmitted through the body using two triaxial accelerometers (EGA3 – 5D for the head and EGA3 – 25D for the shank, Entran, Fairfield, NJ) and 3) the vertical component of the ground reaction force using an instrumented treadmill (Model #9810S1x, Kistler Instrument Corp., Amherst, NY). This enabled characterization of the emergent strategies in the individual subjects during locomotion and active gaze stabilization for the two tasks being tested.

Data Collection

Measurement of Full-Body Kinematic Data

Six time synchronized CCD cameras, sampling at 60 Hz, were used to obtain the three dimensional positions of light weight retro-reflective markers placed on the various body segments. Three cameras fitted with 8 mm lenses were aimed to capture upper body motion data (i.e. waist up) while the remaining three cameras fitted with 6mm lenses were aimed to capture the lower limb motion (i.e. waist down). Each camera in this "two split-body" measurement setup was positioned between 1.8 and 2.5 meters from the center of the calibration volume (each three-camera setup views a calibration volume of 0.75 x 0.50 x 0.98 meters), in a distribution that covered from "two o'clock" to "seven o'clock" in the xy-plane (with 12 o'clock being in the direction of progression). The

characteristics of this measurement system setup have been measured and reported elsewhere (22,23) and are reported here in brief. The actual resolution for this arrangement was calculated to be 0.06mm, but this was rounded up to 0.1mm for practical reporting. This resolution is approximately 0.40% of the marker size (25mm) and 0.02% of the shortest calibration volume dimension (502mm). Based on a worst-case resolution error (0.2 mm) for two markers placed at a minimum distance of 200 mm, the angular resolution was determined to be of the order of 0.06°. Repeatability also was computed to 0.1mm. Accuracy ranged from 0.05mm to 0.16mm. Studies that measure head-trunk kinematics during treadmill locomotion using other optical motion systems have reported similar angular resolution values for their measurement systems (approximately 0.1°, 4). Data collection included a quiet standing trial for a period of 3 seconds to obtain the orientation of the individual body segment axes systems.

Head movements, about and along the three dimensions, were measured with three passive retro-reflective markers affixed to a helmet of negligible mass, approximating the positions of the vertex, above the right tragion and the nuchale of the head. For measurement of trunk movement, subjects wore a T-shaped vest with three markers placed on the superior tip of the spinous process of the C7 vertebra, and at equal distances laterally from the midline at the level of the 10^{th} thoracic vertebra. Data were collected to measure the motion of the right lower limb segment in the sagittal plane. For this purpose, two markers each were affixed to bony landmarks on the lower limb modeled as three segments: thigh, shank and foot. Passive retro-reflective markers were affixed to the femoral greater trochanter, lateral femoral epicondyle, fibular head, lateral malleolus, shoe surface coincident with lateral surface of the calcaneous, the fifth

metatarsophalengeal joint on the superior aspect of the shoe, on the right side of the body. Foot-switches (Motion Lab Systems, Inc., USA) were attached to each shoe at the heel and the toe to enable the determination of heel strike and toe off events. A 12-bit A/D converter at the rate of 60 Hz sampled the footswitch data.

Measurement of Shock-Wave Transmission

The shock transmitted to the head was measured using two sets of triaxial accelerometers packaged in a square box (12mm x 12mm x 12mm). The accelerometer measurement of the head was obtained from the set fixed on to the anteromedial aspect of the helmet worn by the subject during testing. The shank accelerometer measurement was obtained from the set fixed on to the anteromedial aspect of the lower right leg. The measuring axes of both the accelerometers were aligned visually in the sagittal plane such that one of the axes corresponds to the body cranial axis and the other corresponds to the body ventral axis.

Measurement of Ground Reaction Forces

External vertical component of the ground reaction forces for both the right and left foot were measured using a Gaitway™ Instrumented treadmill. The force and accelerometer data were acquired at a sampling rate of 1000 Hz using the Gaitway™ Gait Analysis System and Software.

Data Analysis

Analysis of Number Recognition Data

The responses of the subjects to the numerals presented on the computer were recorded and checked against the numerals that were presented. Percentage correct

numerals were calculated based on the total number of optotypes that were presented per font size.

Analysis of Footswitch Data

The footswitch data from each foot were analyzed to provide the heel strike and toe off information for each gait cycle. One gait cycle was defined as the time when the heel footswitch was turned on by the foot touching the ground to the following heel strike of the same foot. Since the footswitch data were sampled at a rate of 60 Hz, the temporal resolution of the heel strike information was determined to be ±16 ms. In order to simplify the analysis, heel strike and toe off information for 15 consecutive gait cycles per trial during the steady state were used for further analysis. Heel strike and toe off information from both feet were used to calculate the stride time (gait cycle time), step time (heel strike to toe off) and double support time (heel strike of the ipsi-lateral foot to the toe off of the contra-lateral foot) for the two conditions.

Analysis of Kinematic Data

Marker data were processed to derive three-dimensional position information relative to a coordinate frame coincident with the surface of the treadmill using the Motion Analysis System's analysis software (Motion Analysis Corp., Santa Rosa, CA). The marker trajectories were filtered using a fourth order low-pass, zero phase response, Butterworth filter with its cut-off frequency at 6 Hz. A segmental axes system was defined using a right-hand orthogonal system based on bony landmarks obtained during the quiet standing trial and was used to provide a consistent frame of reference independent of body segment position (24). The rotational motion of a body in 3-D space

or relative to another body may be completely and uniquely defined using a transformation matrix between the laboratory inertial axes and a set of body fixed axes or between the two sets of body fixed axes. An eulerian angle convention (22,25) referred to as the gyroscopic system was used to calculate the angular motion about the three axes for the head and trunk segment coordinate systems with respect to the body segment axes defined using the quiet standing trial. The vertical (z-axis) trunk translation was determined from the marker placed coincident with the tip of the C7 spinous process. Each 20-second trial period for each of these movement parameters was subjected to Fourier analysis. The amplitude of the signals in the frequency range of 1.5–2.5 Hz (high frequency) was summed to estimate the predominant contributions of vestibular reflexive mechanisms to head movement control (26,27). The coordination between the head and trunk was measured using the cross correlation function between the head and trunk pitch re space angles as well as that between the head pitch and trunk vertical translation. The temporal variations of the head pitch angular position, trunk pitch angular position and vertical trunk translation were time normalized over the entire gait cycle - heel strike (0%) to the following heel strike (100%) of the right foot - at one percent gait cycle intervals. The cross correlation functions between the head pitch and trunk pitch orientations (HPTP) and the head pitch and trunk vertical translations (HPTV) were determined. The maximum and minimum values closest to the zero phase lag were quantified as the estimate of coordination between the head and trunk pitch orientations and the head pitch and vertical trunk translations, respectively.

The sagittal plane angles of the thigh, shank and foot were calculated using standard, previously established conventions used in the laboratory (28). The knee and

ankle angles were derived from these segment angles and normalized with respect to their quiet standing angles (zero reference angle). Parameters were calculated from the knee and ankle joint angles re space to determine the total movement in the sagittal plane during each gait cycle. For the knee and ankle joints, the total movement of the joint in the window from heel strike to peak knee flexion were calculated to determine the joint responses to the heel strike event of the gait cycle.

Analysis of the Ground Reaction Force Data

In order to assess the ground reaction forces during walking for the two gaze stabilization tasks, the force information for both the right and left leg in the window from the right heel strike to the peak knee flexion during the stance phase of the gait cycle were analyzed. The right foot force data were analyzed to measure the peak force during the loading phase, as well as the loading rate. The left foot force data were analyzed to measure the peak force during its push off phase, as well as the push-off rate. The loading and push-off rates were calculated as the ratio of the difference between the 10% and 90% of the peak loading or push off forces and the difference between the time indices at which these force events occurred.

Analysis of Shock-Wave Transmission Data.

Shank and head peak acceleration amplitudes after the heel strike event were obtained from the acceleration measurement along the cranial axis. The ratio of these two (head/shank) and the time interval between shank and head peak accelerations were calculated to estimate the transmissibility of the shock wave energy from the shank to the head occurring at the heel strike event. In order to assess the contributions of the initial conditions of the knee and ankle joint angles to the transmission of the high-energy

vibrations to the shank and the head, the initial knee (IKA) and ankle angles (IAA) at heel strike were also determined. For the sake of simplifying the analysis these IKA and IAA were normalized such that their quiet standing angles were 180 and 90 degrees, respectively.

Statistical Analyses

To test the hypothesis that changes in the gaze stabilization task will modify the contributions of the different full body systems responsible for gaze stabilization, each variable was tested separately and paired t-tests were performed comparing the dot and the number recognition conditions with a significance level of 0.05. All tests were two-tailed and done using SPSS release 10 software (SPSS Inc., Chicago, IL, 2000).

3. Results

Number Recognition Characteristics

Figure 1 shows the average (± SEM) across subjects of the percentage of correctly identified numerals in the NRT over all the possible presentations (total of 30 per trial) for the different font sizes across subjects. Subjects identified on average 98.3 (± 0.80) % numerals correctly over all the characters and font sizes presented.

Temporal Stride Characteristics

The temporal stride parameters stride time, stance time and double support time were calculated to compare the lower limb performance for the two gaze stabilization tasks. Data in Figure 2 shows the average (± SEM) across subjects for the two gaze stabilization tasks. There was no systematic difference between the two conditions for the stride time ($t(0.05, 8) = -0.722$, $p = 0.491$) or for the stance time parameters ($t(0.05, 8)$

= -1.030, p = 0.333). The double support time for the NRT was significantly greater (t(0.05, 8) = -6.267, p = 0.0001) than the DOT gaze stabilization task.

Head trunk Coordination During Locomotion

Figure 3 (A-C) shows exemplar time series plots of the vertical trunk translation, head pitch angular motion, and the trunk pitch angular motion of a single subject while performing the DOT gaze stabilization task. Figure 3D and 3E show the cross correlation functions between the head pitch and trunk pitch orientations and the head pitch and trunk vertical translation, respectively, over a typical gait cycle for the DOT gaze condition plotted for lags between –30% to +30 % gait cycle interval. Figure 4 (A-C) shows the magnitude of the mean area under the spectral curve (± SEM) across subjects for the head and trunk rotations in the sagittal plane (pitch movements with respect to space) as well as the vertical trunk translations with respect to space, for the two gaze stabilization conditions during walking. The magnitude of the head pitch angular motion for the NRT was significantly greater (t(0.05, 8) = -3.226, p = 0.012) than in the DOT task. There were no systematic differences between the two gaze stabilization conditions for the magnitude of trunk pitch angular motion (t(0.05, 8) = 0.676, p = 0.518) or for the vertical translation of the trunk (t(0.05, 7) = -0.498, p = 0.632).

To determine if patterns of coordination between the head and trunk were changed between the two-gaze stabilization conditions during walking, we performed cross correlation analysis between the head and trunk motion. Figure 4 (D-E) shows the average (± SEM) across subjects of the maximum and the minimum cross correlation values for the HPTP and the HPTV functions, for the two gaze tasks. There were no systematic differences between the two gaze stabilization conditions for the maximum

HPTP (t(0.05, 8) = -0.887, p = 0.401) or the minimum HPTV (t(0.05, 8) = 0.925, p = 0.382).

Lower Limb Joint Angles

Figure 5 (A-F) shows exemplar plots for one subject of the head and shank acceleration along the cranial axis of these segments, the knee and ankle joint angles as well as the vertical component of the ground reaction force of the left and right foot, while performing the DOT gaze stabilization task. These data are time normalized to 500 points over a gait cycle for presentation purposes only (0 % and 100% representing the right foot heel strike event). Note that the event of peak knee flexion is synchronized with the completion of the loading phase of the right leg as well as the time event when the left leg pushes off the support surface.

Figure 6 (A-B) shows the average (± SEM) across subjects of the total movement of the knee and the ankle flexions during the phase from the heel strike to the peak knee flexion during the stance phase of the gait cycle. The magnitude of the total movement of the knee in the sagittal plane for the NRT was significantly greater (t(0.05, 8) = -3.047, p = 0.016) than for the DOT gaze stabilization task. The magnitude of the total movement of the ankle in the sagittal plane for the DOT task was not significantly different (t(0.05, 8) = -1.561, p = 0.157) as compared to the NRT.

Ground Reaction Force Data

Figure 7 shows the average (± SEM) across subjects of the peak vertical force during the loading phase (7A), the pushoff phase (7B), the loading rate (7C) and the pushoff rate (7D). The magnitude of the peak force on the right foot during the loading phase for the NRT was significantly greater (t(0.05, 8) = -2.958, p = 0.018) than for the

DOT task. There were no systematic differences between the two gaze stabilization conditions for the peak force on the left foot during the pushoff phase ($t(0.05, 8) = -1.238$, $p = 0.251$), the loading rate ($t(0.05, 8) = -1.805$, $p = 0.109$) and the push off rate ($t(0.05, 8) = -1.016$, $p = 0.340$).

Modulation of Shockwave Transmission During Locomotion

The data in Figure 5A show the remarkable consistency with which the high-energy accelerations occur at the head after the right and left heel strike event during a gait cycle. The Figure 8A shows the average (± SEM) across subjects of the peak head acceleration along the cranial axis. Accelerometer data from only six subjects were available for analysis. The magnitude of the peak head acceleration for the NRT was nearly significant ($t(0.05, 5) = -2.415$, $p = 0.061$) and less than the DOT gaze stabilization task. Since the magnitude of the peak head accelerations between the two gaze stabilization conditions was close to significance, we further analyzed this parameter on an individual subject level using a 2 tailed independent sample t-tests with equal variances. Four out of the six subjects showed peak head accelerations for the NRT significantly less than the DOT gaze stabilization task (Subject3: $t(0.05,88) = 5.88$, $p = 0.0001$; Subject6: $t(0.05,88) = 10.729$, $p = 0.0001$; Subject7: $t(0.05,88) = 8.948$, $p = 0.0001$; Subject8: $t(0.05,88) = 3.855$, $p = 0.0001$) while two subjects (Subject5: $t(0.05,88) = 0.407$, $p = 0.685$; Subject9: $t(0.05,88) = -1.106$; $p = 0.272$) showed no significant difference between the two tasks.

Figures 8B, 8C and 8D shows the average (± SEM) across subjects of the peak shank accelerations along the cranial axis of the segment, the ratio head/shank and the time lags between the time instances of the two peak accelerations. There were no

systematic differences between the two gaze stabilization conditions for the peak shank acceleration ($t(0.05, 5) = 0.968$, $p = 0.378$), the ratio between the head to shank peak accelerations ($t(0.05, 5) = 0.678$, $p = 0.528$) or the time lags between the occurrences of the peak head and shank accelerations ($t(0.05, 5) = -0.036$, $p = 0.972$).

In order to assess if the knee and the ankle joints had any role in the changes seen in the peak acceleration of the head and the shank after the right leg heel strike, the IKA and the IAA at heel strike, for the corresponding six subjects, were calculated. Figure 8 (E- F) shows the average (± SEM) across subjects for the IKA and the IAA. There was no significant change in the IKA ($t(0.05, 5) = -1.002$, $p = 0.362$) and the IAA ($t(0.05, 5) = -1.316$, $p = 0.245$) between the two gaze stabilization conditions.

4. Discussion

This investigation was designed to evaluate functional modulation of the head-trunk complex and the lower limb apparatus in response to modifications in a gaze stabilization task. The first gaze stabilization task required subjects to simply fixate a point target while walking. The second task required subjects to read numbers, placing increased demands on full-body gaze stabilization mechanisms.

Number recognition proficiency

Subjects showed a remarkable ability to recognize the different numerals presented during the NRT with a high degree of accuracy across the different font sizes as seen in Figure 1. This demonstrated that subjects were performing the NRT with a high level of proficiency.

Temporal stride characteristics

During the NRT, subjects spent significantly greater time in the double support phase of the gait cycle (i.e. when both feet are on the support surface). This was so, despite no change in the stride time and the step time. The double support time was greater by 10% across all subjects while performing the NRT compared to the DOT gaze stabilization task. Spending more time in the double support period would provide greater stability to the upper body during the NRT. Presumably, this strategy was invoked to facilitate number recognition during walking.

Modulation in head movement control

The head pitch angular movement for the NRT was significantly greater than in the DOT gaze stabilization task in the frequency bandwidth of 1.5-2.5Hz. However, the perturbation to the head control system as quantified by the trunk pitch motion as well as the vertical translation of the trunk, in the same frequency bandwidth, remained unchanged for the two gaze stabilization tasks. During walking, subjects control head pitch angular motion to compensate for their vertical translation as seen in the exemplar plots of Figure 3. Also, as seen in Figure 3, the head pitch angular motion is in phase with the trunk pitch angular motion. This is further reflected in the cross correlation functions HPTP (Figure 3D) and HPTV (Figure 3E) that were calculated to quantify the coordination between the head and trunk. The maximum and minimum values of these functions showed that coordination between the head and trunk was not altered for the two gaze stabilization tasks.

Previous investigators have established the function of the vestibular apparatus in head movement control (29,30). Mechanisms such as passive/inertial, reflex and

voluntary, involved in the control of head movement have been the topic of several investigations (20,26,27,31-33). Keshner, et al. (26,27) have hypothesized that the contribution of the control mechanisms in the modulation of head motion is dependent on the frequency content of the self-generated or externally imposed movements. The three main feedback systems recognized in the control of head position are the cervicocollic reflex (CCR), the vestibulocollic reflex (VCR) and the optocollic reflex (OCR) (34). These head stabilization reflexes use input from the somatosensory receptors in the neck musculature, the vestibular systems and the visual systems, respectively. The inputs from these subsystems contribute to the voluntary and reflex responses that are generated in the control of head movements. Keshner and Peterson (26,27) reported that the reflex control mechanisms have their optimal range of operation in the frequency bandwidth of 1.5-2.5 Hz. Recently it has been found that the head pitch motion re space serves to compensate for the vertical translation of the trunk, predominantly produced by the linear vestibulocollic reflex when subjects have walking speeds greater than 1.2 m/s (4). Moreover, the ability to control head motion to achieve gaze stabilization during locomotion was shown to deteriorate in people with abnormal vestibular function and in astronauts returning from spaceflight resulting from increased head instability and impaired visual acuity (1,15,35). This was achieved predominantly through a reduction in the contributions in the reflex control mechanism bandwidth of 1.5-2.5 Hz (1,35). Thus, we infer from the findings of the current study that performing a gaze stabilization task with increased demands for high visual acuity (correctly identifying numerals) fully engaged the reflexive contribution to the control of head movements. These findings

underscore the concept that head movement control during locomotion can be modulated depending on differing gaze demands.

The lower limb acts as a shock absorber during locomotion

As seen in Figure 5, following the heel strike event both legs are on the support surface (the double support period). During this brief period, the right leg goes into flexion while the left leg gets ready to push off from the support surface. The event of the left leg push-off marks the completion of weight transfer from this trailing leg to the leading right leg. This was followed by the single support phase of the right leg. As reported earlier, the threat to gaze stabilization comes not only from the high energy heel strike event of the gait cycle but also the toe off events during walking. This is evidenced by the loss in control at these events in astronauts returning from a short duration exposure to microgravity performing a gaze stabilization task (28,37).

In addition to the modulations in head movement control we also found that, in response to the NRT, the lower body joint motion was also altered. Our data show that, during the stance phase of the gait cycle in the window from heel strike to the peak flexion of the knee, the total movement of the knee was 11% greater while performing the NRT and was significantly different in comparison to the DOT task. At the same time the ankle joint total movement was also on average ~9 % greater while performing the NRT but was not significantly different in comparison to the DOT task. In comparison to the response of the knee and ankle joints, the peak vertical force during the loading phase of the right leg showed significant increases of 5% while performing the NRT as compared to the DOT task. The loading rate also showed average increases of 16% during the NRT compared to the DOT but was not significant. Also, the peak

vertical force during the push off phase (2% average increase during NRT compared to the DOT) and the push-off rate (3% increase during NRT compared to the DOT) of the left leg remained unchanged (See Figure 7).

The increase in knee flexion during the stance phase of the gait cycle has been implicated to function as a shock absorbing mechanism associated with the rapid weight transfer from the trailing to the leading leg (38,39). The increase in knee flexion during the stance phase after the heel strike has been associated with the rapid transfer of weight during the double support phase, thus providing a shock absorbing mechanism after the heel strike event during walking. This may help in damping out any disturbing forces to the head resulting from this rapid weight transfer during the toe-off event of the gait cycle.

Modulation of energy transmission

Figure 5 also show the accelerations along the cranial axis of the head and the shank during a gait cycle for the DOT gaze stabilization task. The acceleration profiles show the consistent peaks occurring in the head and shank soon after the heel strike event of the right leg (0% gait cycle) and in the head after the left leg heel strike event (50% gait cycle) reflecting the perturbations to the head during the two impacts on the support surface during a typical gait cycle. The peak accelerations at the head for the NRT showed a significant decrement of 13.5%, averaged over four of the possible six subjects; with respect to the DOT gaze stabilization task. The peak acceleration of the head along the vertical axis showed a nearly significant ($p = 0.061$) decrease across the entire subject group for the NRT as compared to the DOT gaze stabilization task. The level of significance may have been affected by the availability of accelerometer data from a

reduced number of subjects (6/9). In the current study, the peak acceleration at the head was measured to be reduced to ~60% of that at the shank during walking for the two gaze stabilization tasks. Cappozzo (40) inferred that attenuation of the excessive vibrations to the head was necessary to reduce perturbations to the visual-vestibular system. Vibrations at the head can severely degrade visual acuity (41). These vibrations, as well as inappropriate or disturbed head-trunk or locomotion control strategies, would interfere with the visual-vestibular integration process. As a result, decrements in sensorimotor integration, dynamic visual acuity and balance are outcomes of excessive vibrations being transmitted to the head (5). We infer from the results of the current study that attenuation of the high-energy vibrations transmitted to the head is a factor that is being controlled by a full-body modulation system. The results of the study also showed that the attenuation response is dependent on the goals of the gaze stabilization task.

The attenuation of forces is not simply a matter of the material characteristics of the body. The musculoskeletal system is assembled in a way such that it can filter out certain components of the heel-strike shock-wave to maintain head vibration within the functional limits of the visual-vestibular system (5). Specific coordinated actions of the lower limbs have been shown to contribute to the attenuation process. Although joint configurations and specifically the degree of flexion at the knee at the instant of heel-strike do play a role in attenuating the shock transmitted to the head, Lafortune, et al. (19) found that the initial knee angle had the opposite effect on the shock measured at the shank and the head. These investigators have shown the shock at the head decreased by 45% with a commensurate increase of shank shock by 57% when they varied the initial knee angles from 0 to 40 degrees. They also show a significant reduction in the

head/shank peak ratio. In the current study, however, the IKA and IAA showed no significant changes between the two gaze stabilization tasks. Also, the measured average peak acceleration at the shank as well as the transmissibility of the high-energy transients (as reflected by the ratio of the head/shank peaks) through the body also remained unchanged between the two gaze stabilization tasks. These results indicate that across the two gaze stabilization tasks, the reduction in the peak acceleration at the head for the NRT as compared to the DOT task may not be attributed to the initial joint configurations at the moment of heel strike and implicates the involvement of other mechanisms.

Other factors that may be contributing to the reduction in head peak vertical acceleration as reported in previous investigations include the head-trunk-pelvis configurations (40,42). Recently several studies have shown that a short latency VCR is elicited during sudden head perturbations of linear peak acceleration amplitudes of 1.2g to as low as 0.4g to modulate and dampen the mechanically induced instability of the head (20,43-45). Thus, the reduction seen in the peak acceleration along the vertical axis of the head seen in the present study during the NRT may indicate that the head movement control system indeed modulates the vertical accelerations reaching the head from the high energy phases of the gait cycle as a function of the gaze stabilization task requirements. In this study, we have also found that the head pitch angular movement for the NRT was significantly greater than in the DOT gaze stabilization task. This increase in head movement may also be related to the constraint of reducing the perturbations reaching the head during the high-energy phases of the gait cycle. The acceleration measured by the accelerometer is a function of not only the impact energy but also the angular velocity and the angular position of the segment (19). Hence, we hypothesize

that the head movement dynamics may contribute towards the reduction in the peak head acceleration. This issue is being pursued through other modeling approaches and will be topics of further investigations.

Thus, the body of evidence presented here elucidates the full body contributions to the gaze stabilization system during dynamic motor activities such as locomotion. This work also provides evidence that the CNS produces and optimizes the online modifications of its different elements for the successful completion of any task based on the boundary conditions placed on it (46). Future experiments will further elucidate both the strategic immediate response characteristics of the full body gaze stabilization system along with its adaptive properties.

Acknowledgements

This study was supported in part by a grant from the NSBRI to Jacob Bloomberg (PI). The authors wish to sincerely thank Jeremy Houser, Bergaila Engineering, Houston, TX, Chris Miller, Jason Richards, and Brian Peters, Wyle Laboratories, Houston, TX, for their help with collection and analysis of data collected during this study. We also wish to thank the subjects for contributing their time participating in this study.

Reference

1. Bloomberg JJ, Peters BT, Huebner WP, Smith SL, Reschke MF Locomotor head-trunk coordination strategies following space flight. J Vestib Res 1997; 7:161-177.
2. Crane BT, Delmer JL Human gaze stabilization during natural activities: Translation, rotation, magnification and target distance effects. J Neurophys 1997; 78: 2129-2144.
3. Moore ST, Hirasaki E, Cohen B, Raphan T Effect of viewing distance on the generation of vertical eye movements during locomotion. Exp Brain Res 1999; 129(3):347-61
4. Hirasaki E, Moore ST, Raphan T, Cohen B Effects of walking velocity on vertical head and body movements during locomotion. Exp Brain Res 1999; 127(2):117-30
5. McDonald PV, Bloomberg JJ, Layne CS A review of adaptive change in musculoskeletal impedance during space flight and associated implications for postflight head movement control. J Vestib Res 1997; 7:239-250.
6. Demer JL, Oas JG, Baloh RW Visual-vestibular interaction in humans during active and passive vertical head movement. J Vestib Res 1993; 3:101-114.
7. Demer JL, Viirre ES Visual-vestibular interaction during standing, walking and running. J Vestib Res 1996; 6:295-313.
8. Demer JL, Amjadi F Dynamic visual acuity of normal subjects during vertical optotype and head motion. Investigative Opthalmology & Visual Science 1993; 34(6):1894-1906.
9. Bril B, Ledebt A Head coordination as a means to assist sensory integration in learning to walk. Neurosci Biobehav Rev 1998; 22(4):555-63.

10. Berthoz A, Pozzo T Head and Body coordination during locomotion and complex movements. In: Swinnen SP, Massion J, Heuer H, Casaer P, ed. Interlimb Coordination: Neural, Dynamical, and Cognitive Constraints. Boston, MA: Academic Press; 1994:147-165.

11. Grossman GE, Leigh RJ, Bruce EN, Huebner WP, Lanska DJ Performance of the human vestibulo-ocular reflex during locomotion. J Neurophysiol 1989; 62:264-272.

12. Grossman GE, Leigh RJ, Abel LA, Lanska DJ, Thurston SE Frequency and velocity of rotational and head perturbations during locomotion. Exp Brain Res 1988; 70: 470-476.

13. Pulaski PD, Zee DS, Robinson DA The behavior of the vestibulo-ocular reflex at high velocities of head rotation. Brain Research 1981; 222: 159-165

14. Pozzo T, Berthoz A, Lefort L Head stabilization during various locomotor tasks in humans I. Normal Subjects. Exp Brain Res 1990; 82:97-106.

15. Pozzo T, Berthoz A, Lefort L, Vitte E Head stabilization during various locomotor tasks in humans II. Patients with bilateral peripheral vestibular deficits. Exp Brain Res 1991; 85:208-217.

16. Bloomberg JJ, Reschke MF, Huebner WP, Peters BT The effects of target distance on eye and head movement during locomotion. Ann NY Acad Sci 1992; 656:699-707.

17. Voloshin AS Shock absorption during running and walking, Journal of the American Podiatric Medical Association 1988; 78(6):295-299

18. Valiant GA Transmission and attenuation of heel-strike accelerations, In Biomechanics of Distance Running, ed. P.R. Cavanagh; 1990:225-247.

19. Lafortune MA, Lake MJ, Hennig EM Differential shock transmission response of the human body to impact severity and lower limb posture. J Biomech 1996; 29(12):1531-7

20. Ito Y, Corna S, von Brevern M, Bronstein A, Gresty M The functional effectiveness of neck muscle reflexes for head righting in response to sudden fall. Exp. Brain Res 1997; 117:266-272

21. Holt KG, Jeng SF, Ratcliffe R, Hamill J Energetic cost and stability during human walking at the preferred stride frequency. J Motor Beh 1995; 27:164-178.

22. Mulavara AP, Verstraete MC, Layne CS, McDonald PV, Bloomberg JJ Modulation of Head movement control during walking, Gait & Posture, In Press, 2002.

23. Miller CA, Mulavara AP, Bloomberg JJ A quasi-static method for determining the characteristics of a motion capture camera system in a "split-volume" configuration. Gait and Posture, In Press, 2002.

24. McConville JT, Churchill TD, Kaleps I, Clauser CE, Cuzzi J Anthropometric relationships of body and body segment moments of inertia. Dayton, OH: Wright-Patterson AFB; 1980.

25. Chao EYS Justification of a triaxial goniometer for the measurement of joint rotation. J Biomech 1980; 13:989-1006.

26. Keshner EA, Peterson BW Mechanisms controlling human head stabilization. I. Head-neck dynamics during random rotations in the horizontal plane. J Neurophysiol 1995a; 73:2293-2301.

27. Keshner EA, Cromwell RL, Peterson BW Mechanisms controlling human head stabilization. II. Head-neck characteristics during random rotations in the vertical plane. J Neurophysiol 1995b; 73:2302-2312.

28. McDonald PV, Basdogan C, Bloomberg J, Layne C Lower limb kinematics during treadmill walking after space flight: Implications for gaze stabilization. Exp Brain Res 1996; 112:325-334.

29. Guitton O, Kearney RE, Werely N, Peterson BW Visual, vestibular and voluntary contributions to human head stabilization. Exp Brain Res 1986; 64: 59-69.

30. Goldberg J, Peterson BW Reflex and Mechanical Contributions to head stabilization in alert cats. Journal of Neurophysiology 1986; 56(3): 857-875.

31. Viviani, P, Berthoz A Dynamics of the Head-Neck System in Response to small Perturbations : Analysis and Modeling in the Frequency Domain. Biological Cybernetics 1975; 19:19-37

32. Winters JM. Biomechanical Modeling of the Human Head and Neck. In B. W. Peterson & F. J. Richmond (Eds.), Control Of Head Movement New York Oxford: Oxford University Press; 1988:22-36.

33. Gresty MA Stability of the head: Studies in normal subjects and in patients with labyrinthine disease, head tremor, and dystonia. Movement Disorders 1987; 2(3) : 165-185.

34. Schor RH, Kearney RE, Dieringer N Reflex stabilization of the head. In B. W. Peterson & F. J. Richmond ed. Control of Head Movement, New York: Oxford University Press; 1988.

35. Hillman EJ, Bloomberg JJ, McDonald PV, Cohen HS Dynamic visual acuity while walking in normals and labyrinthine deficient patients. J Vestib Res 1999; 9(1): 49-57

36. Shirley DM, Mulavara AP, Merkle LA, Cohen HS, Bloomberg JJ Varied walking velocities and dynamic visual acuity during locomotion. American Academy of Otolaryngology-Head and Neck Surgery Foundation Annual Meeting, New Orleans, LA; 1999.

37. Layne CS, McDonald PV, Bloomberg JJ Neuromuscular activation patterns during locomotion after space flight. Exp Brain Res 1997; 113:104-109.

38. Gard SA, Childress DS The influence of stance-phase knee flexion on the vertical displacement of the trunk during normal walking. Arch Phys Med Rehabil 1999; 80(1):26-32

39. Sutherland DH, Kauffman KR, Moitoza JR. Kinematics of normal human walking. In: Rose J, Gamble E editors. Human Walking, 2nd ed. Baltimore (MD): Williams & Wilkins; 1994:23-44.

40. Cappozzo A, Figura F, Leo T, Marchetti M Movements and mechanical energy exchanges in the upper part of the human body during walking. In: E. Asmussen & K. Jorgensen (Eds.), Biomechanics VI-A. Baltimore: University Park Press; 1978:272.

41. Griffin MJ, Lewis CH A review of the effects of vibration on visual acuity and cotinuous manual control. Part 1: Visual Acuity. J Sound Vibration 1978; 46:269-276.

42. Thorstensson A, Nilsson J, Carlson H, Zomlefer MR Trunk movements in human locomotion. Acta Physiol Scand 1984; 121:9-22.

43. Allum JH, Gresty M, Keshner E, Shupert C The control of head movements during human balance corrections. J Vestib Res 1997; 7(2-3):189-218.

44. Ito Y, Corna S, von Brevern M, Bronstein A, Rothwell J, Gresty M. Neck muscle responses to abrupt free fall of the head: comparison of normal with labyrinthine-defective human subjects. J Physiol 1995; 489:911-6

45. Aoki M, Matsunami K, Han X, Yamada H, Muto T, Ito Y Neck muscle responses to abrupt vertical acceleration in the seated human. Exp Brain Res 2001; 140(1):20-4.

46. Berstein, NA The Coordination and Regulation of Movements. Pergamon, New York; 1967.

Figure Legends:

Figure1: Percentage correct response to the NRT averaged (± SEM) across subjects over all possible presentations as a function of the font size.

Figure 2: Average (± SEM) across subjects of A) Stride time B) Stance time C) Double support time, for the two gaze stabilization conditions. The '*' denotes significance at $p<0.05$.

Figure 3: Exemplar time series plots from a typical subject for the DOT gaze stabilization task of A) Vertical torso translation with respect to space B) Head angular pitch (extension/flexion) orientation in the sagittal plane with respect to space and C) Torso angular pitch (extension/flexion) orientation in the sagittal plane with respect to space D) The cross correlation function between the head pitch re space and trunk pitch re space (HPTP) over a gait cycle for lags ranging from –30% to +30% gait cycle interval; E) the cross correlation function between the head pitch re space and vertical trunk translation re space (HPTV) over a gait cycle for lags ranging from –30% to +30% gait cycle interval.

Figure 4: Average (± SEM) across subjects of the sum of magnitude under the spectral curve in the 1.5-2.5 Hz bandwidth for A) Head angular pitch (extension/flexion) orientation in the sagittal plane with respect to space B) Vertical trunk translation with respect to space C) Torso angular pitch (extension/flexion) orientation in the sagittal plane with respect to space; D) the maximum correlation coefficient of the cross correlation function between the head pitch re space and trunk pitch re space (HPTP); E) the minimum correlation coefficient of the cross correlation function between the head pitch re space and vertical trunk translation re space (HPTV). The '*' denotes significance at $p<0.05$.

Figure 5) Exemplar plots of the A) the head acceleration along its vertical axis B) the shank acceleration along its vertical axis C) the knee joint orientation with respect to space D) the ankle joint orientation with respect to space D) the vertical component of the ground reaction force measured for the left foot E) the vertical component of the ground reaction force measured under the right foot; for a typical subject performing the DOT gaze stabilization task. Data from 15 gait cycles during a typical trial are overlaid and were time normalized to 500 points with 0% and 100% representing the right foot heel strike event. The shaded regions are the double support phases when both feet are on the ground.

Figure 6: The average (± SEM) across subjects of the total movement calculated from the heel strike to the peak flexion of the knee during the stance phase for A) the ankle joint and B) the knee joint, for the two gaze stabilization tasks. The '*' denotes significance at $p<0.05$.

Figure 7: The average (± SEM) across subjects of the peak vertical force during A) the loading phase, B) the push-off phase, C) the loading rate and D) the push-off rate. The '*' denotes significance at $p<0.05$.

Figure 8: The average (± SEM) across the six of nine subjects of the A) peak acceleration at the head, B) the peak acceleration at the shank, C) the ratio of peak acceleration of head/shank, D) the time lag between the occurrences of the peak head and shank accelerations E) the angle of the knee at the heel strike event F) the angle of the ankle at the heel strike event.

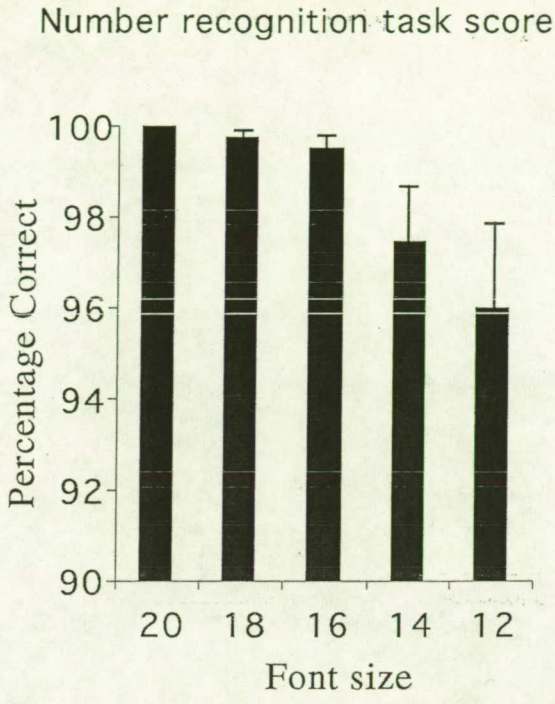
Number recognition task score
Percentage Correct
100
98
96
94
92
90
20
18
16
14
12
Font size

FIGURE 1 : Identifying head-trunk and lower limb contributions to gaze stabilization during locomotion

. Mulavara, [redacted] . and Bloomberg

A) Stride Time

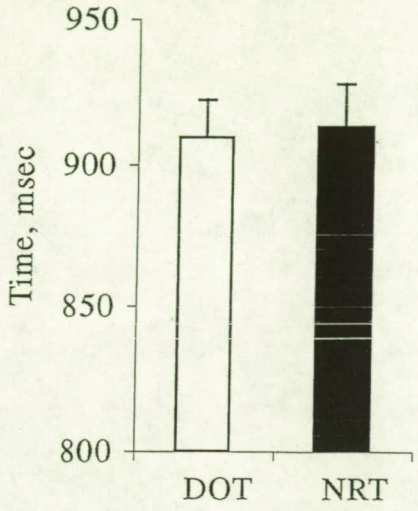

B) Stance Time

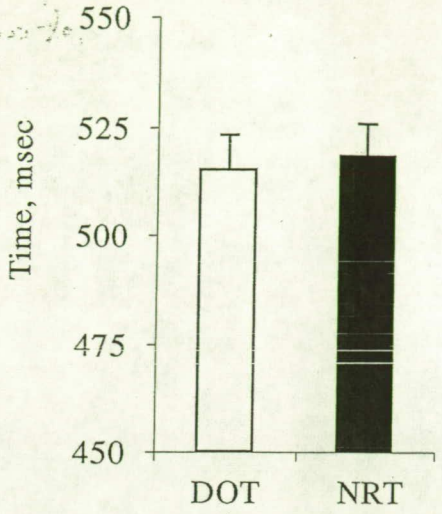

C) Double Support Time

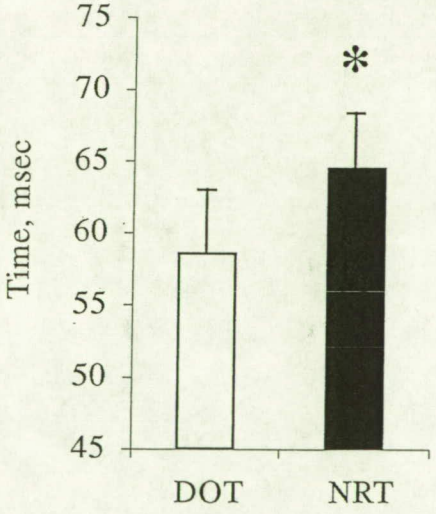

Figure 2: Identifying head-trunk and lower limb contributions to gaze stabilization during locomotion

Mulavara . and Bloomberg

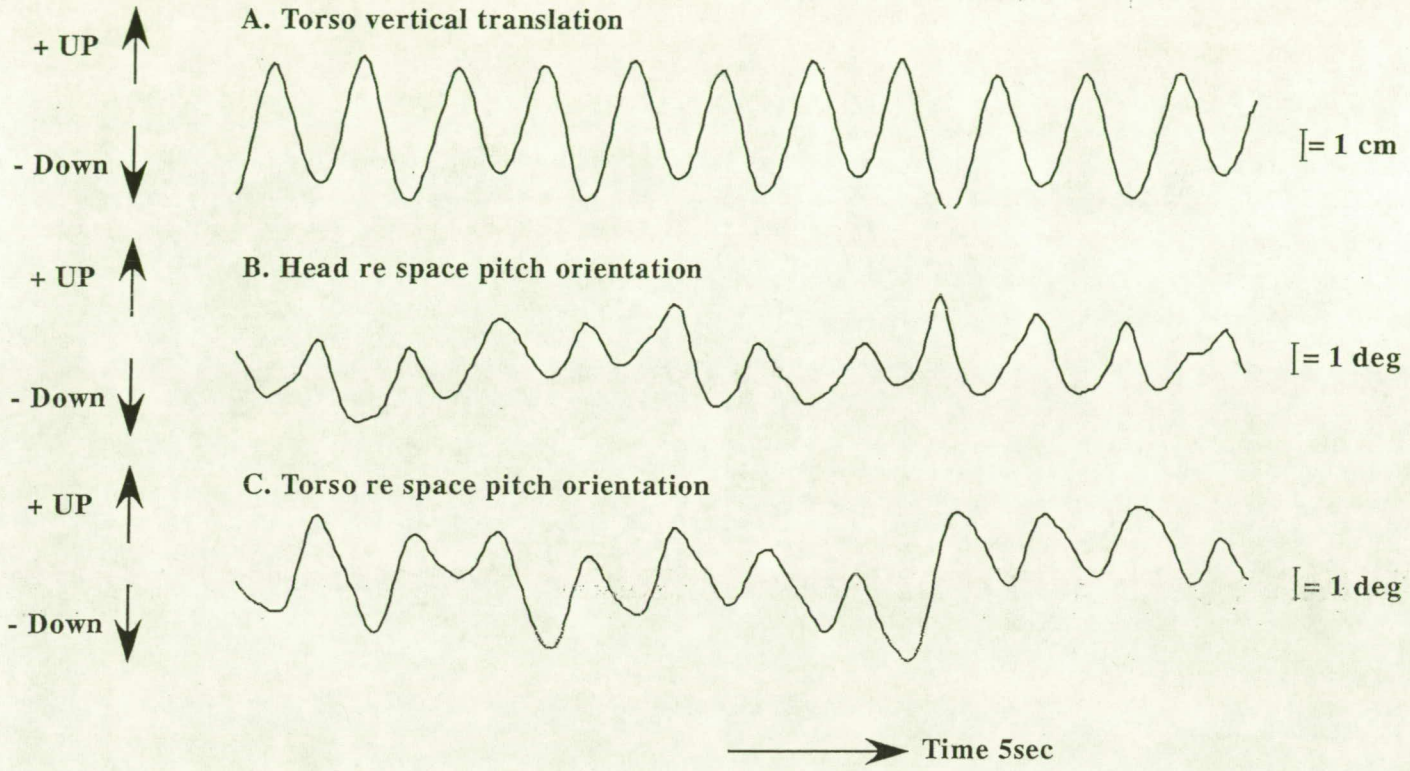

D) Cross correlation function
Head-pitch and Trunk-pitch

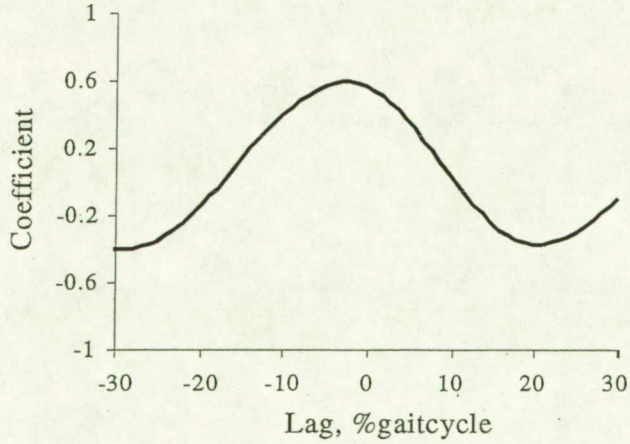

E) Cross correlation function
Head-pitch and Trunk-vertical translation

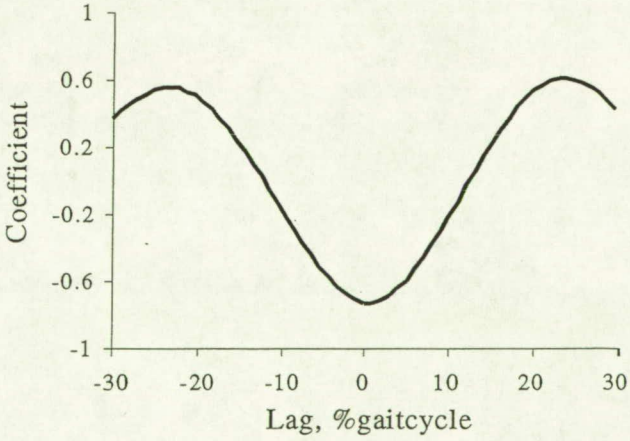

Figure 3: Identifying head-trunk and lower limb contributions to gaze stabilization during locomotion

Mulavara and Bloomberg.

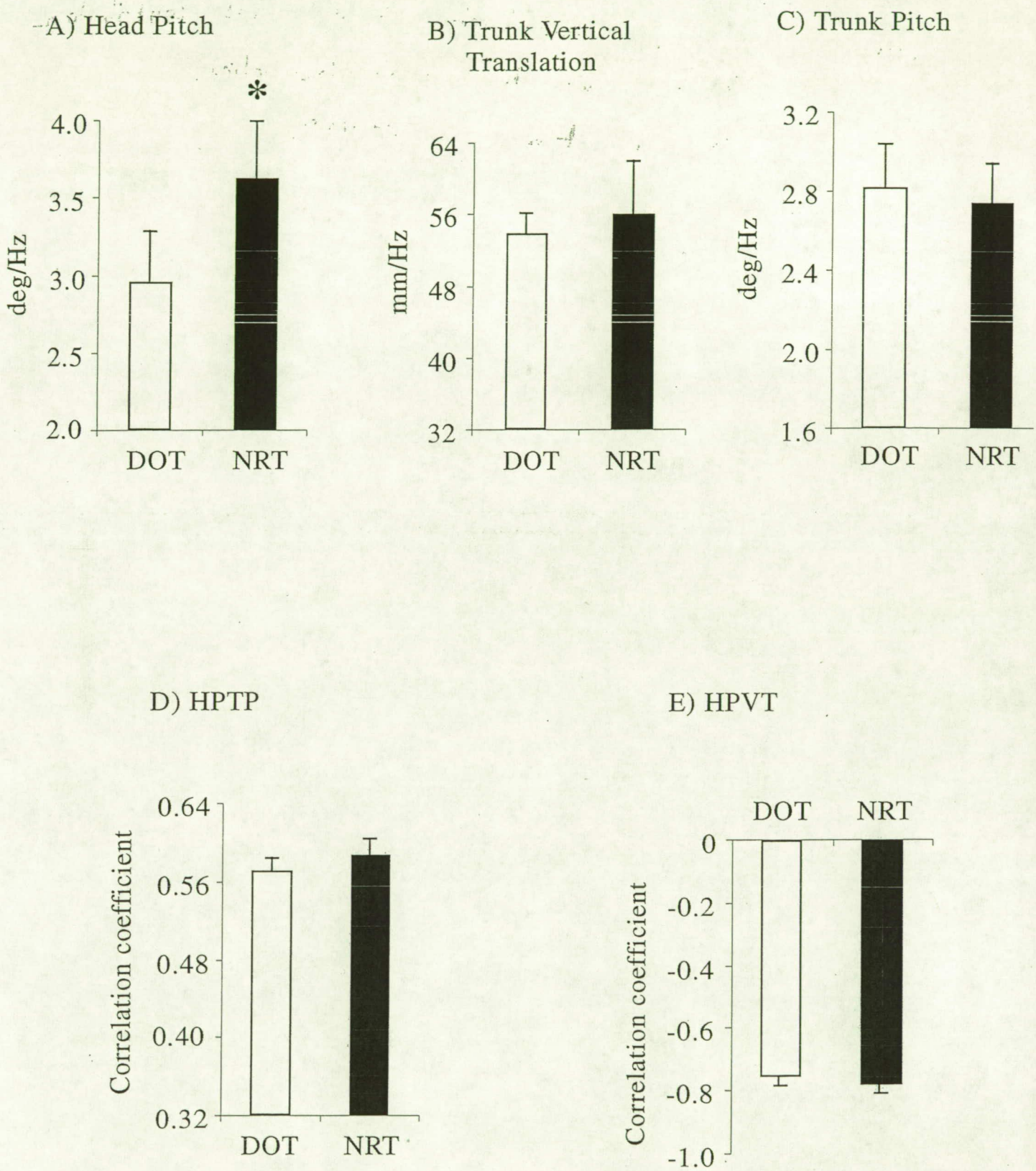
A) Head Pitch
*
4.0
3.5
3.0
2.5
2.0
deg/Hz
DOT
NRT
B) Trunk Vertical Translation
64
56
48
40
32
mm/Hz
DOT
NRT
C) Trunk Pitch
3.2
2.8
2.4
2.0
1.6
deg/Hz
DOT
NRT
D) HPTP
0.64
0.56
0.48
0.40
0.32
Correlation coefficient
DOT
NRT
E) HPVT
DOT
NRT
0
-0.2
-0.4
-0.6
-0.8
-1.0
Correlation coefficient

Figure 4: Identifying head-trunk and lower limb contributions to gaze stabilization during locomotion

Mulavara, [illegible] and Bloomberg

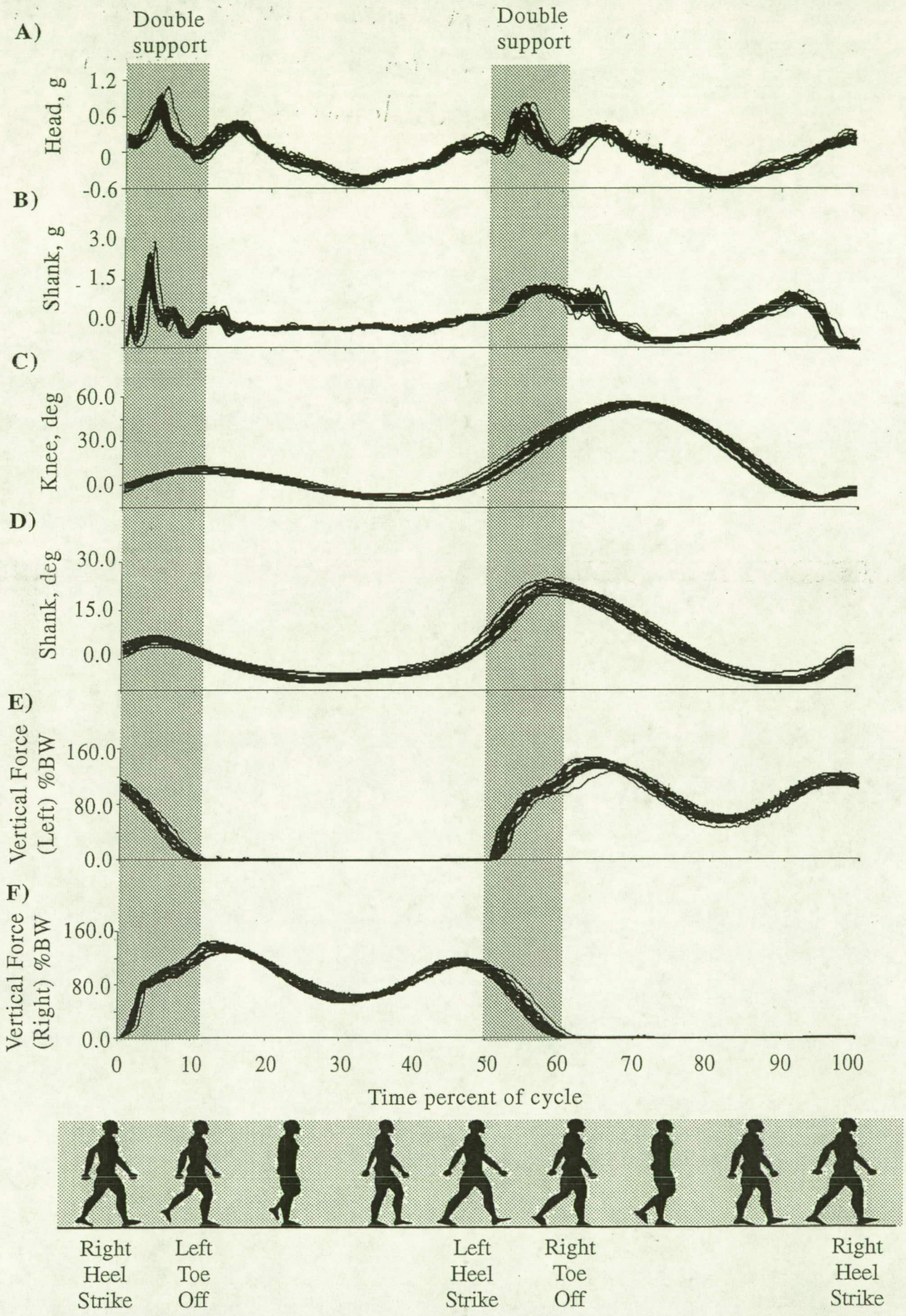
A)
Double support
Double support
Head, g
1.2
0.6
0
-0.6
B)
Shank, g
3.0
1.5
0.0
C)
Knee, deg
60.0
30.0
0.0
D)
Shank, deg
30.0
15.0
0.0
E)
Vertical Force (Left) %BW
160.0
80.0
0.0
F)
Vertical Force (Right) %BW
160.0
80.0
0.0
0
10
20
30
40
50
60
70
80
90
100
Time percent of cycle
Right Heel Strike
Left Toe Off
Left Heel Strike
Right Toe Off
Right Heel Strike

Figure 5 : Identifying head-trunk and lower limb contributions to gaze stabilization during locomotion

Mulavara and Bloomberg

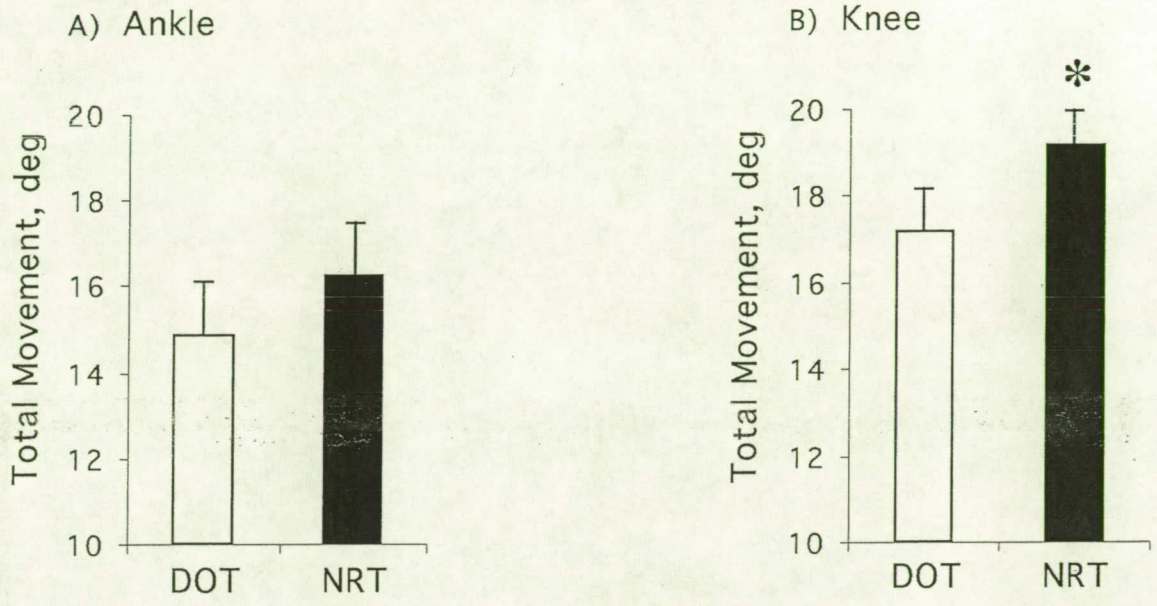
A) Ankle
Total Movement, deg
20
18
16
14
12
10
DOT
NRT
B) Knee
*
Total Movement, deg
20
18
16
14
12
10
DOT
NRT

Figure 6 : Identifying head-trunk and lower limb contributions to gaze stabilization during locomotion

Mulavara and Bloomberg

A) Right foot

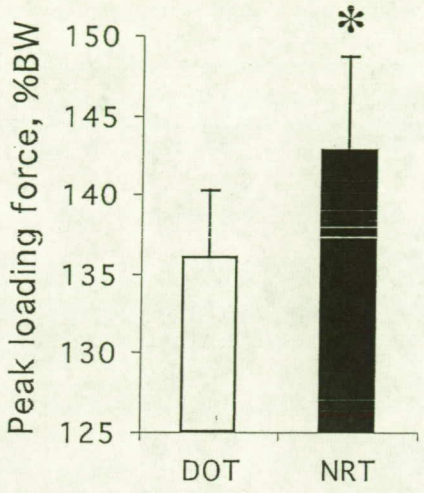

B) Left foot

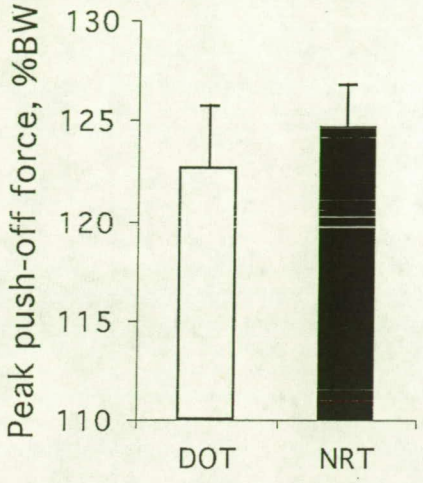

C) Right foot

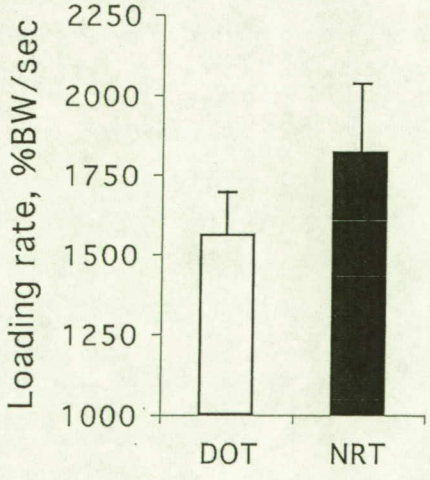

D) Left foot

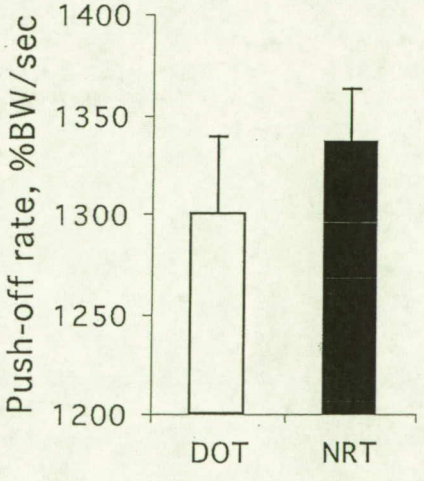

Figure 7: Identifying head trunk and lower limb contributions to gaze stabilization during locomotion Mulavara and Bloomberg.

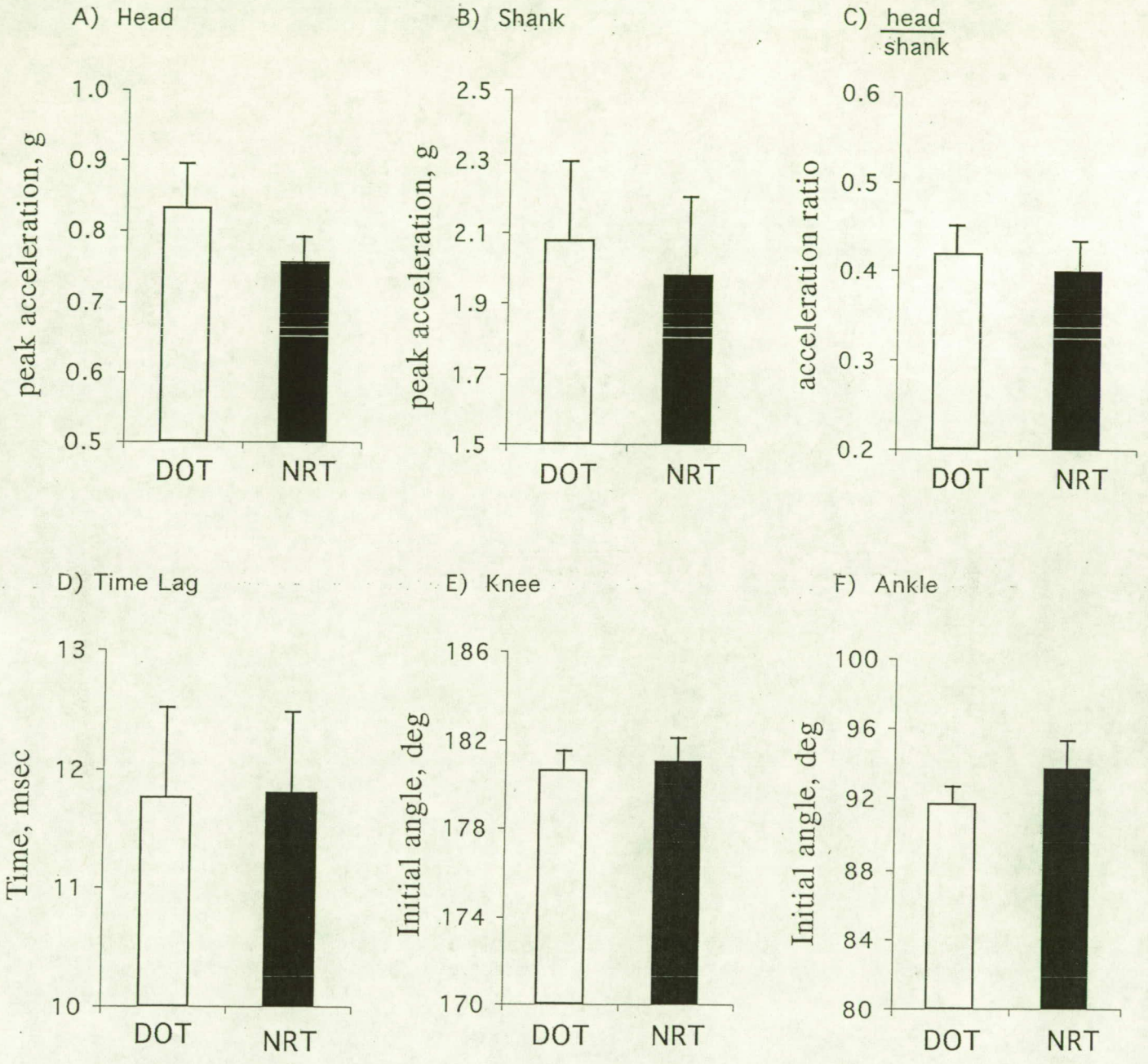
A) Head
peak acceleration, g
1.0
0.9
0.8
0.7
0.6
0.5
DOT
NRT
B) Shank
peak acceleration, g
2.5
2.3
2.1
1.9
1.7
1.5
DOT
NRT
C) head / shank
acceleration ratio
0.6
0.5
0.4
0.3
0.2
DOT
NRT
D) Time Lag
Time, msec
13
12
11
10
DOT
NRT
E) Knee
Initial angle, deg
186
182
178
174
170
DOT
NRT
F) Ankle
Initial angle, deg
100
96
92
88
84
80
DOT
NRT

Figure 8: Identifying head-trunk and lower limb contributions to gaze stabilization during locomotion
Mulavara and Bloomberg.